Molecular Neurobiology (2019) 56:6324–6340
https://doi.org/10.1007/s12035-019-1519-0

Transferrin Enhances Microglial Phagocytic Capacity

Tomás R. Carden[1] · Jorge Correale[2] · Juana M. Pasquini[1] · María Julia Pérez[1]

Received: 18 October 2018 / Accepted: 29 January 2019 / Published online: 13 February 2019

Abstract

Transferrin (Tf) is a glycoprotein playing a critical role in iron homeostasis and transport and distribution throughout the body and within tissues and cells. This molecule has been shown to accelerate the process of myelination and remyelination in the central nervous system (CNS) in vivo and induce oligodendroglial cell maturation in vitro. While the mechanisms involved in oligodendroglial precursor cell (OPC) differentiation have not been fully elucidated yet, our group has previously described the first molecular events taking place in OPC in response to extracellular Tf. Here, we show the effect of Tf on the different glial cell populations. We demonstrate that, after a CNS demyelinating injury, Tf can be incorporated by all glial cells—i.e., microglia, astrocytes, and OPC—and that, acting on microglial cells in vitro, Tf increases microglial proliferation rates and phagocytic capacity. It may be then speculated that the in vivo correlation of this process could generate a favorable microenvironment for OPC maturation and remyelination.

Keywords Transferrin · Microglial phagocytosis · Demyelination · Remyelination · Astrocytes

Abbreviations

aTf	Human apotransferrin
BrdU	Bromodeoxyuridine
CC	Corpus callosum
CD11b	Cluster of differentiation 11b (integrin alpha M)
CNS	Central nervous system
CPZ	Cuprizone
Ctl	Control
Cyt B	Cytochalasin B
EIA	Enzyme immunoassays
FCS	Fetal calf serum
GFAP	Glial fibrillary acidic protein
Griffonia	Griffonia simplicifolia isolectin B4
Hoechst	bisbenzimide H-33258
HRP	Horseradish peroxidase
ICI	Intracranial injection
IL	Interleukin
LPS	Lipopolysaccharide
MBP	Myelin basic protein
MS	Multiple sclerosis
MTT	Thiazolyl blue tetrazolium bromide
NG2	Neural/glial antigen 2
OLG	Oligodendrocyte
OPC	Oligodendrocyte precursor cells
PDGFR-α	Platelet-derived growth factor receptor-alpha
PFA	Paraformaldehyde
PI	Propidium iodide
Tf	Transferrin
TfR	Tf receptor 1
Tf-TR	Human Tf conjugated to Texas Red
TNF-α	Tumor necrosis factor alpha

✉ María Julia Pérez
mjperez@ffyb.uba.ar

[1] Departamento de Química Biológica e Instituto de Química y Fisicoquímica Biológica "Prof. Alejandro C. Paladini" (IQUIFIB), Facultad de Farmacia y Bioquímica (FFyB), Consejo Nacional de Investigaciones Científicas y Técnicas (CONICET), Universidad de Buenos Aires (UBA), Junín 965, CABA, Buenos Aires, Argentina

[2] Instituto de Investigaciones Neurológicas "Dr. Raúl Carrea", FLENI, Buenos Aires, Argentina

Introduction

Microglia are myeloid cells in the central nervous system (CNS) parenchyma which are regarded as both glial cells and mononuclear phagocytic cells involved in inflammatory and immune responses [1, 2] and whose function is to protect the CNS from injury. Microglial cells also exhibit an important role during development and regenerative processes, including wrapping and removing damaged cell debris after brain injury [3, 4], secreting growth factors [5, 6], and engaging in synaptic pruning [7]. However, they are also implicated

in the pathogenesis of inflammatory demyelinating diseases, such as multiple sclerosis (MS), via the secretion of toxic molecules and antigen presentation to lymphocytes [8]. Increased levels of proinflammatory factors such as interleukin (IL)-1, IL-6, tumor necrosis factor alpha (TNF-α), and other indicators of microglial activation have been correlated with neurodegenerative diseases including Alzheimer's disease and traumatic brain injury [9]. In this context, several lines of evidence indicate that microglia and their products can cause neuronal damage [10, 11] by driving a chronic inflammatory reaction and thus contribute to the process of neuropathological changes in different neurodegenerative diseases.

Demyelination involves either in situ microglial activation and proliferation [12] or, in the case of neuroinflammation, the recruitment of lymphocytes and monocytes from circulation [13]. Microglial activation is accompanied by an increase in the expression of myeloid markers CD11b and ED1 and morphological changes such as cell soma enlargement and process retraction and shortening. Following these morphological changes and as a consequence of activation, amoeboid microglia become round-shaped and exhibit phagocytic capacity [14].

Microglia can adopt different states of activation depending on the type, context, and duration of the stimulus, with M1 and M2 representing a wide spectrum of diverse phenotypes with specific functional significance rather than two different cell subtypes [8, 15–17]. Although there are many caveats to the M1/M2 terminology, it nevertheless provides useful terms to identify different microglia contributions [18, 19]. As the classic proinflammatory phenotype, M1 microglia are in charge of removing pathogens by recognizing toll-like receptors and secreting TNF-α, IL-1, IL-6, and oxygen/nitrogen species [20, 21]. In contrast, phagocytic M2 microglia are sub-classified into M2a, M2b, or M2c in the absence of inflammation [22, 23] and induce a Th2-like response. Key microglial functions during remyelination include favoring OPC differentiation, removing myelin debris, and releasing trophic factors [19, 24, 25]. In other words, the characteristics adopted by microglia during demyelination and remyelination are fundamental aspects of successful CNS regeneration [18, 26].

Over the last decade, there has been a surge of interest in the study of astrocytes in health and disease. In contrast to earlier reports describing astrocytes only as stable cells providing mainly structural and metabolic support and contributing to the blood-brain barrier, it has now become clear that astrocytes also carry out a range of homeostatic maintenance functions [27]. Indeed, in MS lesions, astrocytes exert dual and paradoxical roles during disease development [28, 29].

Tf is the main Fe^{3+} transporter in the organism and is mostly expressed in the liver. Moreover, Tf mRNA expression is known to increase after birth, which indicates an important role for Tf in development [30]. Regarding its role in remyelination strategies, our group has previously reported that a single intracranial injection (ICI) of apotransferrin (aTf) in 3-day-old rats increases the expression of diverse myelin constituents [31–34]. In addition, our in vivo findings were reproduced in oligodendrocyte (OLG) primary cultures and in N19 and N20.1 cell lines. These results are in line with studies showing that aTf regulates myelin basic protein (MBP) transcription and enhances myelinogenesis in myelin-deficient rats by synergizing with EGF-1 [35–41].

In this context, the aim of the present work is to evaluate the effects of aTf treatment on microglial cells to create a favorable condition that allows OPC differentiation. In vivo experiments showed that all glial cells incorporate Tf after a cuprizone (CPZ)-induced demyelinating lesion, while in vitro assays revealed that the target phenotype into which microglial cells differentiate is modulated by Tf, increasing their proliferation rate and phagocytic capacity.

Materials and Methods

Materials

Human aTf, CPZ, paraformaldehyde (PFA), serum albumin, poly-L-lysine, triiodothyronine (T3), Triton X-100, and bisbenzimide H-33258 (Hoechst) were obtained from Sigma-Aldrich (St Louis, MO, USA). DMEM/F12 and human Tf conjugated to Texas Red (Tf-TR) were from Life Technologies (Carlsbad, CA, USA). Fetal calf serum (FCS) was from Cripion (Sao Paulo, Brazil). Mowiol was from Calbiochem (Nottingham, UK). Immobilon-P^{sq} (PVDF transfer membrane) was from Millipore (Temecula, CA, USA). Hyperfine ECL and ECL Plus Western Blotting Detection Reagents were from GE Healthcare (Buckinghamshire, UK). All other chemicals were of analytical grade.

Antibodies used were rabbit anti-myelin basic protein (MBP) (a generous gift from A. Campagnoni-UCLA); mouse anti-glial fibrillary acidic protein (GFAP; Sigma-Aldrich); mouse anti-CD11b OX-42 and rabbit anti-NG2 chondroitin sulfate proteoglycan (Millipore); mouse anti-CNPase and goat anti-platelet-derived growth factor receptor α (PDGFR-α; Neuromics, Edina, MN, USA); mouse anti-CD71 OX-26 Tf receptor (BD Biosciences Pharmingen, San José, CA, USA); mouse anti-bromodeoxyuridine (BrdU; Roche, Basel, Switzerland); biotinylated *Griffonia simplicifolia* lectin 1 isolectin B4 (Vector Laboratories, Burlingame, CA, USA); and rhodamine phalloidin (Molecular Probes, Invitrogen, Carlsbad, CA, USA). Horseradish peroxidase (HRP)-, Cy2-, DyLight 488-, Cy3-, and DyLight 549-conjugated secondary antibodies were obtained from Jackson ImmunoResearch Laboratories (West Grove, PA, USA).

Animal Treatment

All animal procedures were held following the guidelines established by the Committee of Bioethics, at Facultad de Farmacia y Bioquímica, Universidad de Buenos Aires (CICUAL Exp 0006360/15; Res. 2429/15). Newly born Wistar rats were housed under 12-h light/dark cycles. At post-natal day 21 (P21), a randomly selected group was fed a standard powdered rodent chow carefully mixed with 0.6% CPZ (bis (cyclohexanone)oxaldihydrazone; *w*/*w*) during 2 weeks to induce demyelination, while another group was fed a control diet. At P35, the CPZ group was returned to a control diet.

Tf Incorporation In Vivo Assays

At P35, animals were administered an ICI of 350 ng aTf in a volume of 1 μl saline solution [31]. Controls were injected the same volume of saline solution. Injections were stereotaxically applied in the corpus callosum (CC) with a glass capillary at 0.25 μl/min during 2 min. Coordinates were 1 mm lateral from the midline, 2 mm posterior from the bregma, and 2.2 mm deep from the dura mater [42]. In another set of experiments, control and demyelinated rats were injected Tf-TR at P35 using the same coordinates described for aTf injection. After 24 h, animals were sacrificed, tissue samples were obtained, and brain slices with positive red signal (Tf-TR) were processed as described below for Tf incorporation analysis in the different CNS glial cells by confocal microscopy.

Tissue Preparation and Immunohistochemistry

At P35 and P36, animals were anesthetized with 75 mg/kg ketamine and 10 mg/kg xylazine and perfused through the left heart ventricle with PBS followed by PFA 4% in PBS. Brains were carefully removed and fixed overnight in PFA 4% at 4 °C, and later cryoprotected by extensive immersion in 15% and 30% sucrose in PBS at 4 °C. Finally, a set of brain tissue samples was frozen with freezing spray and stored at − 80 °C until processed, while another set was used to obtain 20-μm cryostat tissue sections which were conserved in 50% glycerol at − 20 °C until processed. For floating immunohistochemistry assays, sections were washed in PBS, permeabilized with 0.1% Triton X-100 in PBS, and blocked with 5% FCS in PBS. Two different controls were carried out: (a) no primary antibody control, sample incubated with antibody solution followed by incubation with corresponding secondary antibody; (b) isotype control, tissue incubated with the same host of the primary antibody in blocking solution followed by incubation with corresponding secondary antibody. For histochemistry assays, brain slices were rinsed three times in PBS, mounted onto gelatin-treated glass slides, and air dried. Sections were blocked in 5% FCS–PBS solution for 2 h, then sequentially exposed to the primary and secondary antibodies, and finally mounted with Mowiol mounting solution. Additionally, 20-μm brain sections placed directly on gelatin-treated glass slides. After air drying, sections were soaked in PBS, dehydrated in 70% ethanol, stained with 0.5% Sudan black in 70% ethanol for 30 min, and, finally, rinsed with water. Images were observed in fluorescence Olympus BX50 or a confocal Olympus FV1000 microscope (Olympus, Tokyo, Japan). Fluorescence microscopy images were analyzed using Image-Pro Plus 5.5 software (Media Cybernetics, Rockville, MD, USA), while confocal microscopy images were analyzed using Fluoview 2.1 software (Olympus). Immunohistochemistry for each marker was performed in triplicate from at least three independent experiments.

Microglial Primary Cultures

Primary cultures of microglial cells from newborn Wistar rats were performed according to McCarthy and de Vellis [43]. After removing the meningeal membranes, newborn rat cerebral hemispheres were mechanically dissociated in a mixture of DMEM/F12 (1:1 *v*/*v*) containing 20 μg/ml streptomycin and 20 U/ml penicillin, supplemented with 10% FCS. Cell suspensions were seeded in poly-L-lysine-coated 75-cm^2 tissue culture flasks and incubated at 37 °C in 5% CO_2, with medium changes every 3 days. When cells reached confluence, the microglial subpopulation was obtained after 140 rpm/min shaking during 1 h. More than 96% of the isolated microglial cells were CD11b-positive. Cell suspension was centrifuged at 300×*g* for 10 min and the pellet resuspended in DMEM/F12 (1:1 *v*/*v*) with 10% FCS. Cells were cultured either on 12-mm coverslips or 30-mm Petri dishes during 24 h.

Astroglial Primary Culture

Primary cultures of mixed glial cells were shaken overnight on an orbital shaker at 250 rpm at 37 °C. The suspended cells were discarded and attached cells were then detached with 0.25% trypsin after rinsing briefly with 0.2% ethylenediaminetetraacetic acid. Cells were plated in 96-well plates in DMEM/F12 (1:1 *v*/*v*) supplemented with 10% FCS and 1% penicillin-streptomycin during 1 day. Then, astroglial cells were treated for 2 days. The culture contained around 85% $GFAP^+$ cells, a specific marker for astrocytes.

Culture Treatment

According to experiments, the microglial or astroglial medium was changed to DMEM/F12 (1:1 *v*/*v*) with 1% FCS after 24 h in DMEM-F12 supplemented with 10% FCS. Then, cells

were cultured in basal conditions or activated by 10 ng/ml lipopolysaccharide (LPS) during different times in the presence or absence of 100 μg/ml aTf. Microglial cells were also incubated with 100 μg/ml Tf-TR for 30 min at 37 °C. After being washed, cells were fixed and Tf incorporation was analyzed by fluorescence microscopy.

Cell Viability Assays

Microglial cells were seeded in 96-well plates and incubated with 0.5 mg/ml thiazolyl blue tetrazolium bromide (MTT) substrate for 1 h at 37 °C 5% CO_2 before the end of treatment. MTT cleavage to insoluble formazan crystals (mainly by mitochondrial dehydrogenases) is an indirect measure of cell metabolic activity. After the addition of a 10% SDS 0.1 N HCl solution, absorbance at 570 nm was measured in FlexStation equipment.

Cell Death and Nitrite Assays

Microglial cells were exposed to a 100 μg/ml propidium iodide (PI) solution for 30 min after treatment and analyzed by microscopy. Cells incorporating the fluorescent PI dye were considered dead cells. After microglia treatments, culture media were collected and total nitrites present in the media were evaluated following the Griess technique [44]. Briefly, 50 μl of 6.5 M HCl and 50 μl of 37.5 mM sulphanilic acid were added to 200 μl of culture media. After 10 min of incubation at 4 °C, 50 μl of 12.5 mM NED was added. After 30 min of incubation at 4 °C, samples were centrifuged (6700×*g*) for 10 min at 4 °C. A standard curve was generated with sodium nitrite with concentrations ranging from 1 to 100 μM. Absorbance at 540 nm was measured in a spectrophotometer.

Cell Proliferation Assays

BrdU incorporation was evaluated by enzyme immunoassays (EIA) and immunocytochemistry. BrdU (10 μM) was added to the culture media during treatment in order to label cells in the S phase. For EIA, cells were incubated with a mouse antibody anti-BrdU (1:1000) during 1 h at 37 °C in 0.1% Triton X-100 in PBS with 1% FCS and then with an anti-mouse antibody conjugated to HRP during 1 h at 37 °C. After washing three times with PBS, the enzymatic reaction was carried out during 30 min using 3,3′,5,5′-tetramethylbenzidine (TMB) as substrate, and the kinetic reaction was stopped using 1 M phosphoric acid. Absorbance at 450 nm was measured in FlexStation equipment. Immunocytochemical analyses were conducted as described below.

Phagocytosis Assays

Microglial cells were incubated with *Saccharomyces cerevisiae* conjugated with FITC at the end of treatment for 15 min at 37 °C. Two different phagocytosis controls were carried out: (a) incorporation in the presence of 1 and 10 μM cytochalasin B (Cyt B) for the inhibition of actin polymerization and (b) temperature variation at 4 °C before yeast-FITC addition and then the assay done at 4 °C. Phagocytic particles were quantified by fluorescent microscopy to be expressed as the number of particles internalized per cell. Nuclei were identified with Hoechst [45–47].

Immunocytochemistry

Microglial cells were fixed with 4% PFA in PBS for 15 min at room temperature, permeabilized, and blocked with 5% FCS in 0.01% Triton X-100 PBS solution for 2 h. Cells were then incubated overnight at 4 °C with the following primary antibodies: anti-MBP, anti-NG2, anti-PDGFR-α, anti-CD71, *Griffonia simplicifolia*, anti-CD11b, anti-GFAP, anti-BrdU, and rhodamine phalloidin. Coverslips were then rinsed, incubated for 2 h at room temperature with the appropriate fluorescent-conjugated secondary antibodies, and, finally, mounted with Mowiol solution. Two different controls were carried out: (a) no primary antibody control, sample incubated with antibody solution followed by incubation with corresponding secondary antibody; (b) isotype control, cells incubated with the same host of the primary antibody in blocking solution followed by incubation with corresponding secondary antibody. Images were examined in an epifluorescence Olympus BX50 microscope or a confocal Olympus FV1000 microscope. Epifluorescent images were analyzed with Image-Pro Plus software (Media Cybernetics) and confocal images were analyzed using Fluoview 2.1 software (Olympus). Nuclei were identified with Hoechst to determine the total number of cells in each slide [48]. Positive cells for each antibody were normalized to Hoechst-positive cells in each condition and quantified using Image-Pro Plus 4.5 software.

Statistical Analysis

Infostat software was used to determine if the data set is normally distributed. Graph-Pad Prism software was used for data analysis of three independent experiments. Results are presented as the mean ± SEM. Comparisons were made using two-way ANOVA, followed by Neuman-Keuls post-tests for multiple comparisons; $***p < 0.001$, $**p < 0.01$, $*p < 0.05$; ns non-significant.

Results

Tf Cell Targets After CPZ-Induced Demyelination In Vivo

Brain tissue coronal sections (Fig. 1a) obtained from P35 control and CPZ-treated rats were used to evaluate demyelination in the CC. Sudan black and Eriochrome-cyanine R assays showed lower staining in the CC of CPZ animals, along with a decrease in CC size as a consequence of demyelination (Fig. 1b and c). The loss of immunoreaction for oligodendroglial markers MBP and CNPase was also observed after CPZ intoxication (Fig.1d). In addition, astrogliosis was detected through GFAP expression and microgliosis was observed through the use of CD11b (Fig.1e).

Animals intoxicated with CPZ were injected Tf-TR in order to determine whether glial cells other than OLG are targets for Tf incorporation in demyelinated animals. Reconstructed confocal images of CC revealed that OPC, identified through PDGFR-α, incorporated Tf in control as well as in demyelinated rats (Fig. 2a and b). OPC red fluorescence was concentrated in the intracellular region close to the nucleus, a characteristic feature of endocytosis. Astrocytes identified through GFAP expression revealed a red punctate mark along processes in demyelinated animals, which was absent in control animals (Fig. 2c and d). Finally, microglial cells identified by CD11b expression were able to incorporate Tf in both control and demyelinated rats (Fig. 2e and f). Red fluorescence was observed in cell processes but particularly cell nuclei. As microglia are phagocytic cells, Tf is probably incorporated faster than in other glial cells and, once inside the cell, Tf-TR molecules are degraded, which allows their diffusion to the cell nuclei.

Effects of Tf Treatment on Microglia In Vitro

Microglia primary culture characterization rendered 96.4% $CD11b^{+}$/*Griffonia*$^{+}$ cells identified as microglial cells (Fig.3a–c), 2.3% $NG2^{+}$/PDGFR-α^{+} or double positive cells identified as OPC (Fig. 3d–f), and 1.33% $GFAP^{+}$ cells identified as astrocytes (Fig. 3g and h). *Griffonia*$^{+}$ cells were found to express Tf receptor 1 (TfR) (Fig. 4a–c) and to incorporate Tf-TR (Fig. 4d–f). After Tf-TR incorporation, immunodetection of type 1 TfR was evaluated again, with results rendering 99.7% TfR^{+}/Tf-TR^{+} cells with the punctate pattern characteristic of the membrane receptor. Red

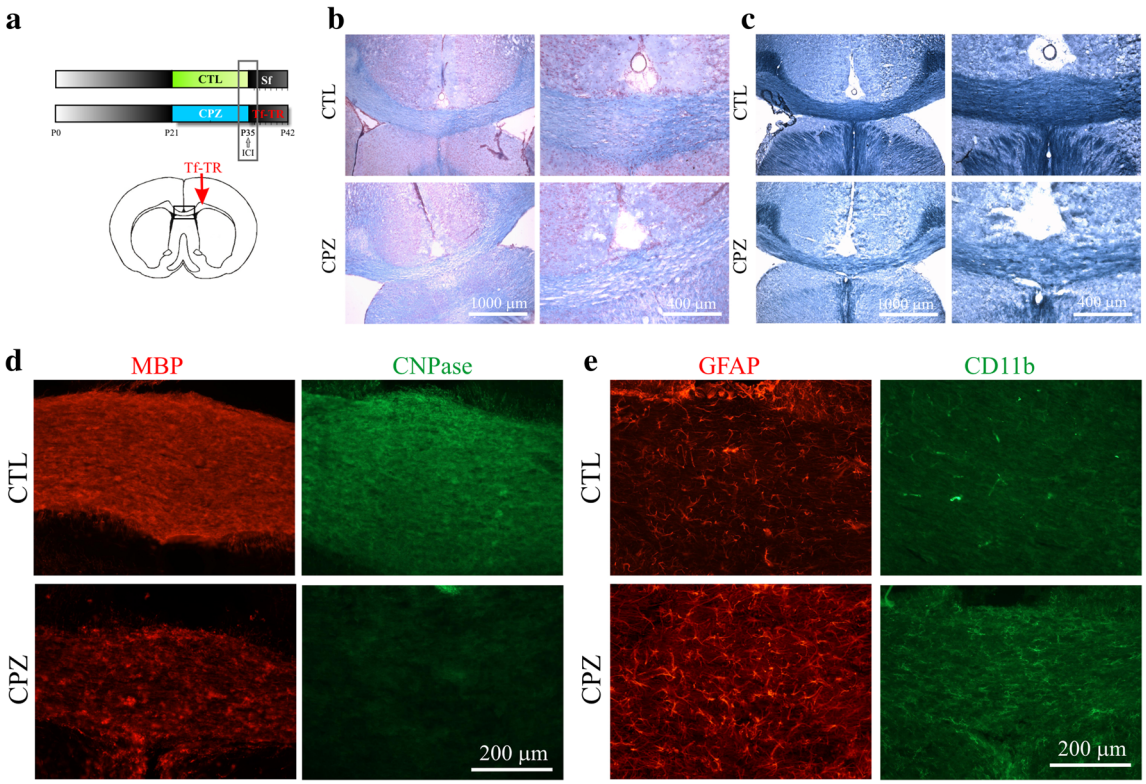

Fig. 1 Cuprizone-induced demyelination in vivo. **a** Schematic representation of the experimental design and rat brain coronal slice indicating the area analyzed in the corpus callosum. Histological analyses of CTL and CPZ animals at P35 using **b** eriochrome-cyanine R staining; **c** Sudan black B staining; **d** oligodendroglial marker MBP (red) and CNPase (green) staining; **e** astroglial marker GFAP (red) and microglial marker CD11b (green) staining. Scale bars, 1000 µm for left images **b** and **c**, 400 µm for right images **b** and **c**, 200 µm for images **d** and **e**. CD11b: cluster of differentiation 11b (integrin alpha M); CPZ: cuprizone; CTL: control; GFAP: glial fibrillary acidic protein; ICI: intracranial injection; MBP: myelin basic protein; Sf: physiological solution; Tf-TR: Texas red-labeled transferrin

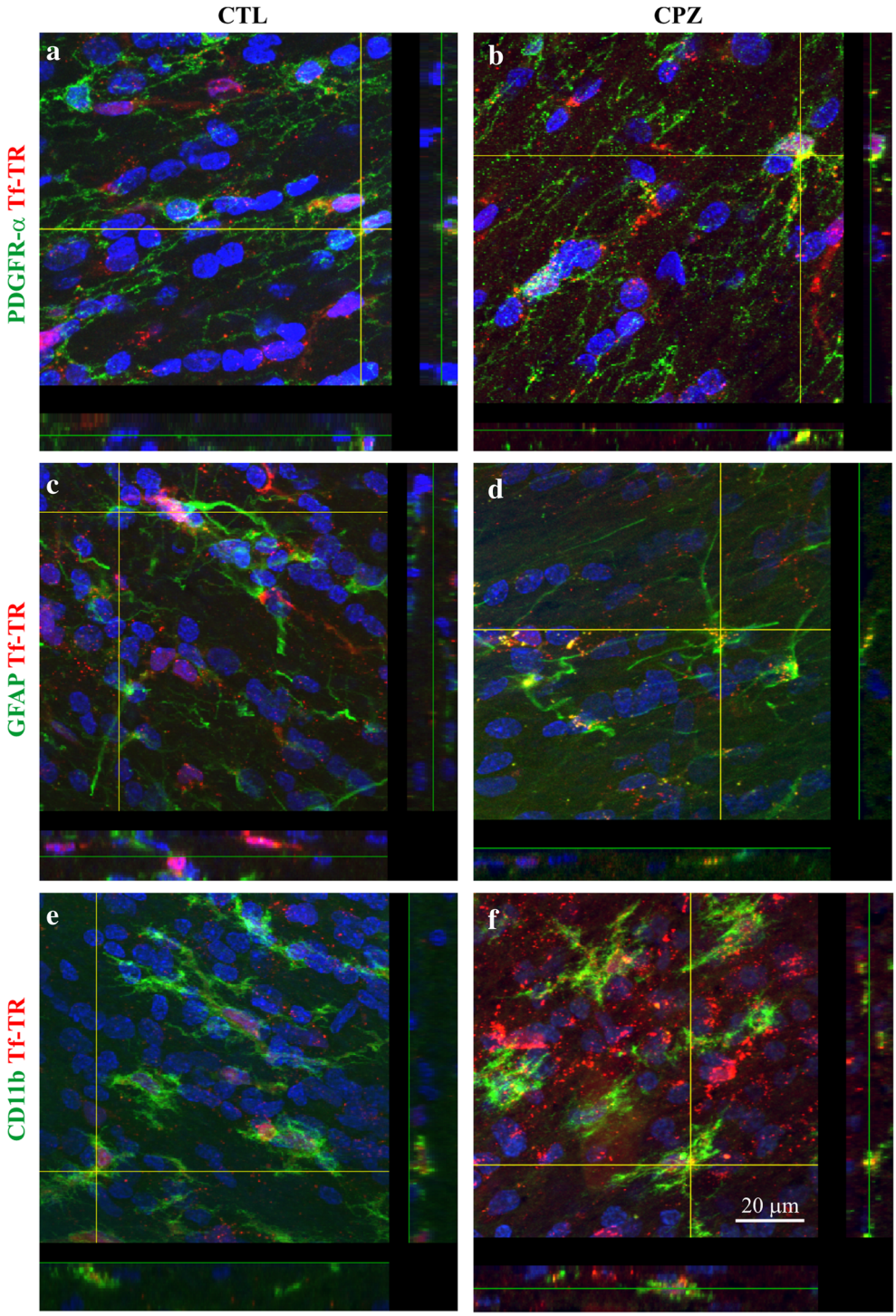

Fig. 2 Tf-TR incorporation in glial cells in vivo. Confocal reconstructions of *z*-stack images obtained from CTL and CPZ animals injected Tf-TR (red) at P35 and immunostained 24 h later using **a** and **b** oligodendroglial cell marker PDGFR-α (green); **c** and **d** astrocyte marker GFAP (green); **e** and **f** microglial marker CD11b (green); nuclear staining using Hoechst (blue). Full-stack images, x–z (bottom margin box) and y–z (right margin box) planes of triple labeling on the selected yellow line intersections. Scale bar, 20 μm for all images in the panel. CD11b: cluster of differentiation 11b (integrin alpha M); CPZ: cuprizone; CTL: control; GFAP: glial fibrillary acidic protein; PDGFR-α: platelet-derived growth factor receptors - alpha; Tf-TR: Texas red-labeled transferrin

fluorescence corresponding to Tf-TR after 30 min of treatment was observed in the cell soma, indicating endocytic incorporation (Fig. 4g–i).

Microglia viability exposed to the different culture conditions was evaluated by the MTT assay after 12, 24 and 48 h of treatment. The presence of aTf was found to increase cell viability in basal and LPS-activated culture conditions (Fig. 5a–c) at all times analyzed. Subsequent studies to determine the cell mechanisms at play—proliferation or death—were conducted after 48 h of treatment, as this was the condition revealing the sharpest increase in cell viability. Proliferation assays showed a significant increase in $BrdU^+$ cells related to total cells and clear nuclear immunolabeling in the presence of aTf as compared to control conditions. The mere presence of aTf increased cell proliferation by 193.44% related to control, similar to LPS treatment, while LPS

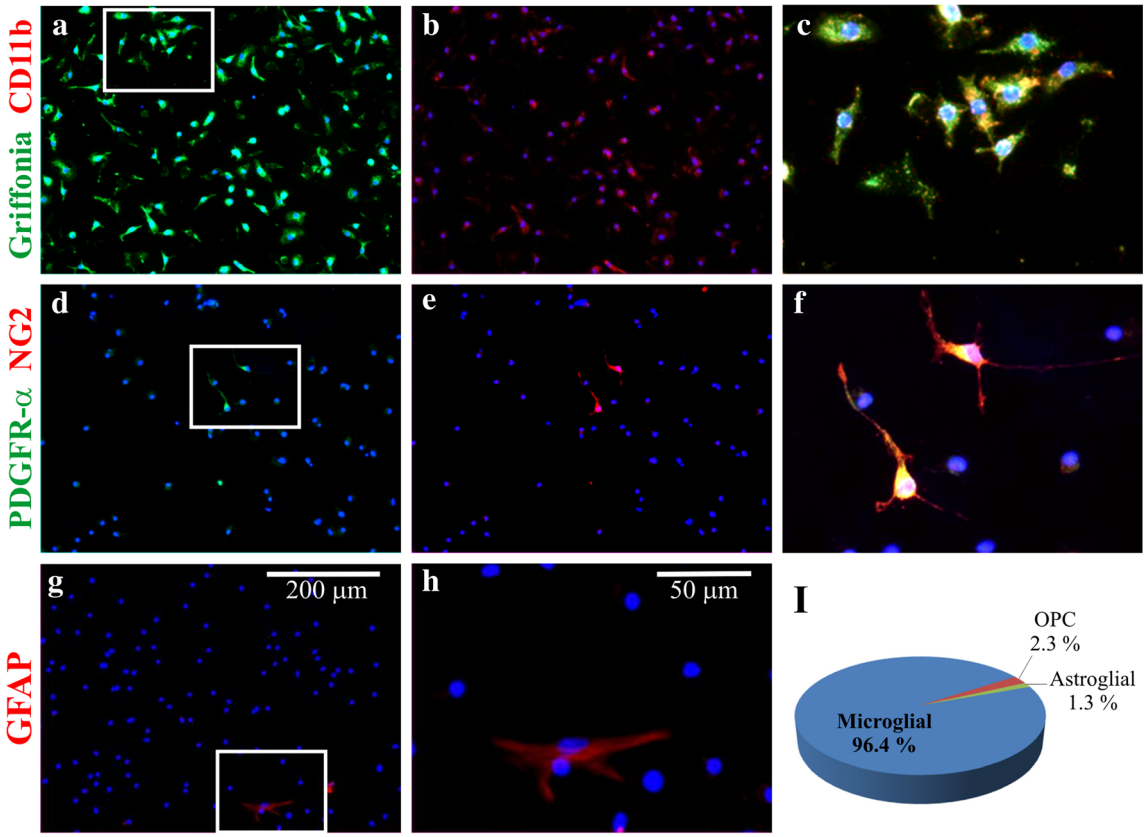

Fig. 3 Culture characterization. Culture purity assessment through immunocytochemistry using **a** to **b** microglial markers *Griffonia simplicifolia* (green) and CD11b (red); **d** to **f** oligodendroglial cell markers PDGFR-α (green) and NG2 (red); **g** and **h** astrocyte marker GFAP (red); nuclear staining using Hoechst (blue). Scale bars, 200 μm for images **a**, **b**, **d**, **e**, and **g**, 50 μm for images **c**, **f**, and **h**. Images **f** and **h** show fields which contain positive cells which are not representative of its percentage in the culture. Images **c**, **f**, and **h** show higher magnification images of insets in **a**, **d**, and **g**, respectively. **i** Quantification of positive cells relative to total nuclei. CD11b: cluster of differentiation 11b (integrin alpha M); GFAP: glial fibrillary acidic protein; Griffonia: *Griffonia simplicifolia* isolectin B4; MBP: myelin basic protein; NG2: neural/glial antigen 2; OPC: oligodendrocyte precursor cells; PDGFR-α: platelet-derived growth factor receptors-alpha

stimulation in the presence of aTf had synergistic effects on BrdU incorporation (Fig. 6a and b). In addition, EIA quantification of the amount of BrdU incorporated revealed significant differences which resembled immunocytochemical findings (Fig. 6c). In turn, cell death evaluated through nuclear PI incorporation was not affected by aTf treatment but significantly increased by LPS as compared to control. Such increase was abolished when LPS treatment was combined with aTf, reaching values close to control conditions (Fig. 7a and b).

Effects of Microglial Tf Treatment on Astrocytes

As mentioned above, microglial primary cultures included a small proportion of other glial cells, which was 1.33% for astrocytes at the beginning of treatment (Fig. 3i). To assess the astrocyte population following changes in microglial phenotypes upon aTf treatment, we studied the proportion of astrocytes after 2 days in the different culture conditions. aTf treatment did not modify the percentage of $GFAP^+$ cells relative to total cells in basal conditions (Fig. 8a and b). However, LPS in the absence of aTf treatment after 2 days showed a significantly lower percentage of astrocytes, from 8.3% in control conditions to 2.8% under LPS activation, while the combination of LPS and aTf rendered a $GFAP^+$ cell proportion similar to that of control conditions (Fig. 8c–e). Worth mentioning, isolated pure cultures of astrocytes were not sensitive to stimulation with aTf, LPS or their combination (Fig. 8f).

Effects of Microglial Tf Treatment on OLG

Microglial cultures also included 2.3% OPC at the beginning of treatment (Fig. 3i). Using the strategy described above, we evaluated changes produced in OLG by shifts in microglial phenotypes. Results showed a higher proportion of MBP^+ cells, from 3.7% in control conditions to 6.9% in the presence of aTf for 2 days (Fig. 9a and b). LPS activation produced a significant decrease of 1.6%inMBP^+ cells and their morphology during LPS treatment was characteristic of dead cells (Fig. 9c). LPS activation combined with aTf produced a return to normal values (Fig. 9d and e).

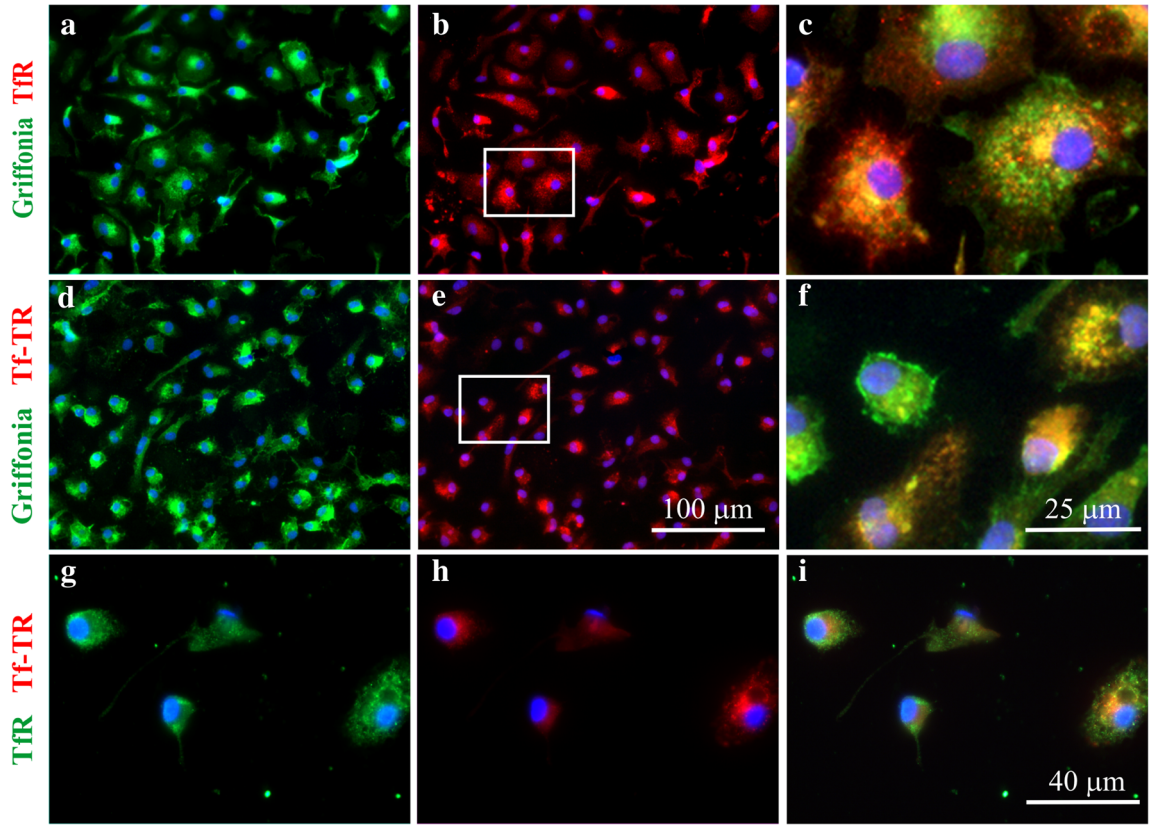

Fig. 4 Tf-TR incorporation and Tf receptor 1 expression in microglial cells in vitro. Immunocytochemical assays in microglial cultures using **a** to **c** Griffonia (green) and an antibody against Tf receptor 1 (red); **d** to **f** Griffonia (green) and Tf-TR (red); **g** to **i** an antibody against Tf receptor 1 (green) and Tf-TR (red); nuclear staining using Hoechst (blue). Scale bars, 100 µm for images **a**, **b**, **d**, and **e**, 25 µm for images **c** and **f**, 40 µm for images **g** to **i**. Merge images **c** and **f** show higher magnification images of insets in **b** and **e**. Griffonia: *Griffonia simplicifolia* isolectin B4; TfR: Tf receptor 1; Tf-TR: Texas red-labeled Tf

Effects of Tf Treatment on Microglial Phagocytic Capacity In Vitro

Microglial phagocytic capacity was analyzed using *Saccharomyces cerevisiae* labeled with FITC after 48 h of treatment. Results obtained in cells activated with LPS in the presence of aTf showed increased phagocytic capacity regarding controls (Fig. 10a–d and l). Control assays using a 10 µM dose of Cyt B inhibited phagocytosis but affected cell survival, while 1 µM showed clear phagocytosis inhibition without affecting cell survival. The second control assay was done at 4 °C, which decreased cell activity and, hence, cell phagocytic capacity (Fig.10e–g). Rhodamine-conjugated phalloidin labeling during assays showed actin cytoskeleton participation in the phagocytic process, with regions of high concentration in areas where yeast phagocytosis took place near the membrane inside the cell, which indicates complete phagocytosis. Of note, multiple long membrane processes

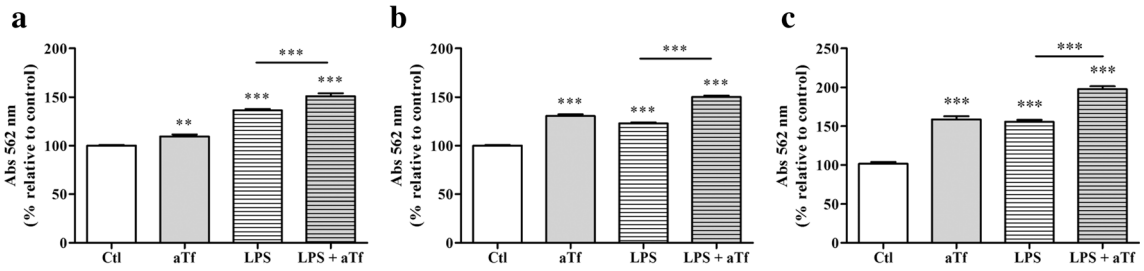

Fig. 5 Microglial cell viability upon aTf treatment. MTT assays in microglial cultures after **a** 12 h, **b** 24 h, and **c** 48 h of aTf treatment in the presence or absence of LPS. Data are presented as the mean ± SEM of three independent experiments using one-way ANOVA followed by Neuman-Keuls multiple comparison test; $***p < 0.001$, $**p < 0.01$, symbols above the bars indicate significance compared to corresponding control. aTf: human apotransferrin; Ctl: control; LPS: lipopolysaccharide

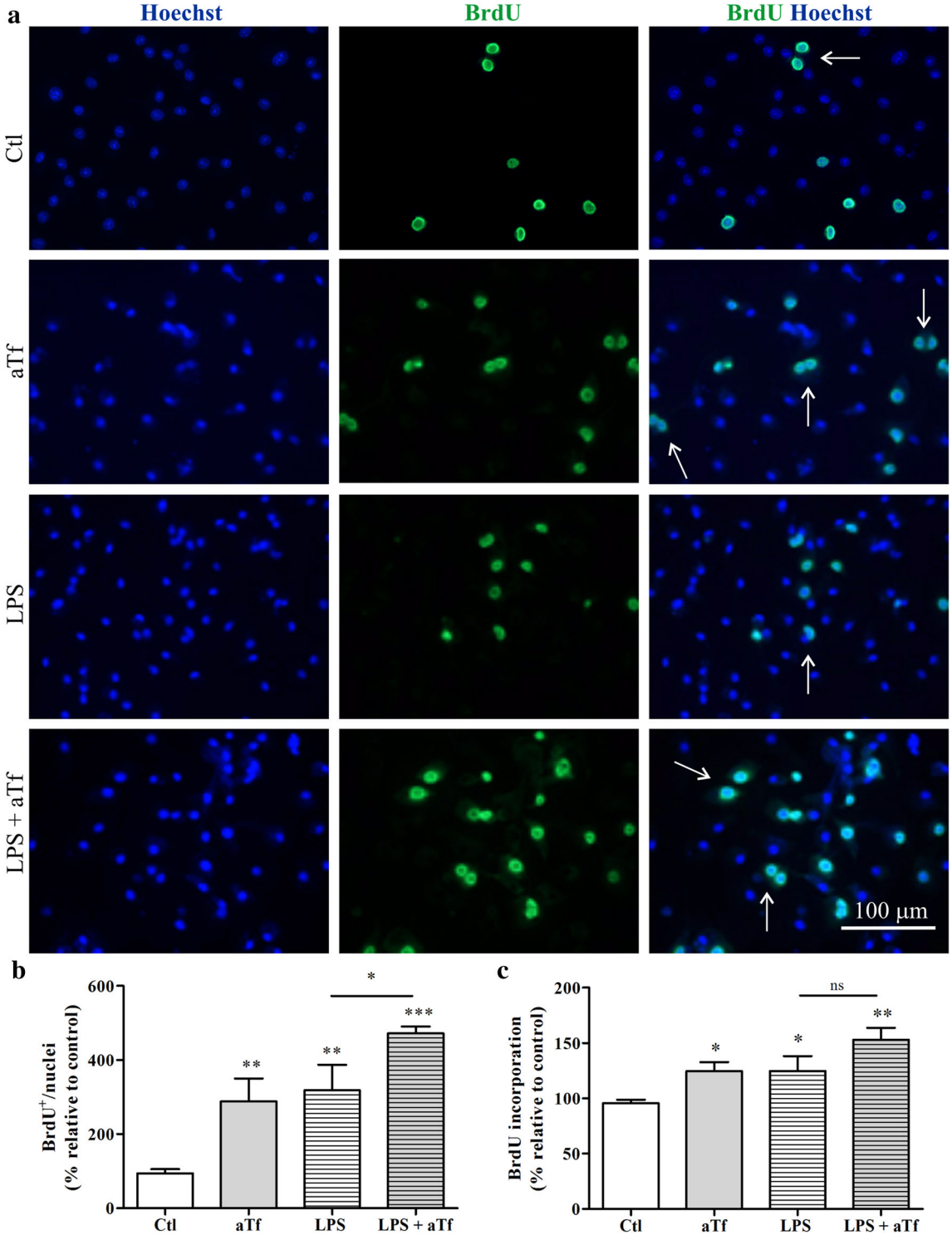

Fig. 6 Microglial cell proliferation upon aTf treatment. **a** Immunnofluorescence analysis of BrdU incorporation (green) in microglial cultures after 48 h of aTf treatment in the presence or absence of LPS; nuclear staining using Hoechst (blue). Two nearby $BrdU^+$/Hoechst cells are indicated with arrows. Scale bar, 100 µm for all images in the panel. **b** Quantification of $BrdU^+$ cells relative to total nuclei; **c** Quantification of BrdU incorporation by enzyme immunoassays (EIA). Data are presented as the mean ± SEM of three independent experiments using one-way ANOVA followed by Neuman-Keuls multiple comparison test; $***p < 0.001$, $**p < 0.01$, $*p < 0.05$, ns non-significant, symbols above the bars indicate significance compared to corresponding control. aTf: human apotransferrin; Ctl: control; LPS: lipopolysaccharide; BrdU: bromodeoxyuridine

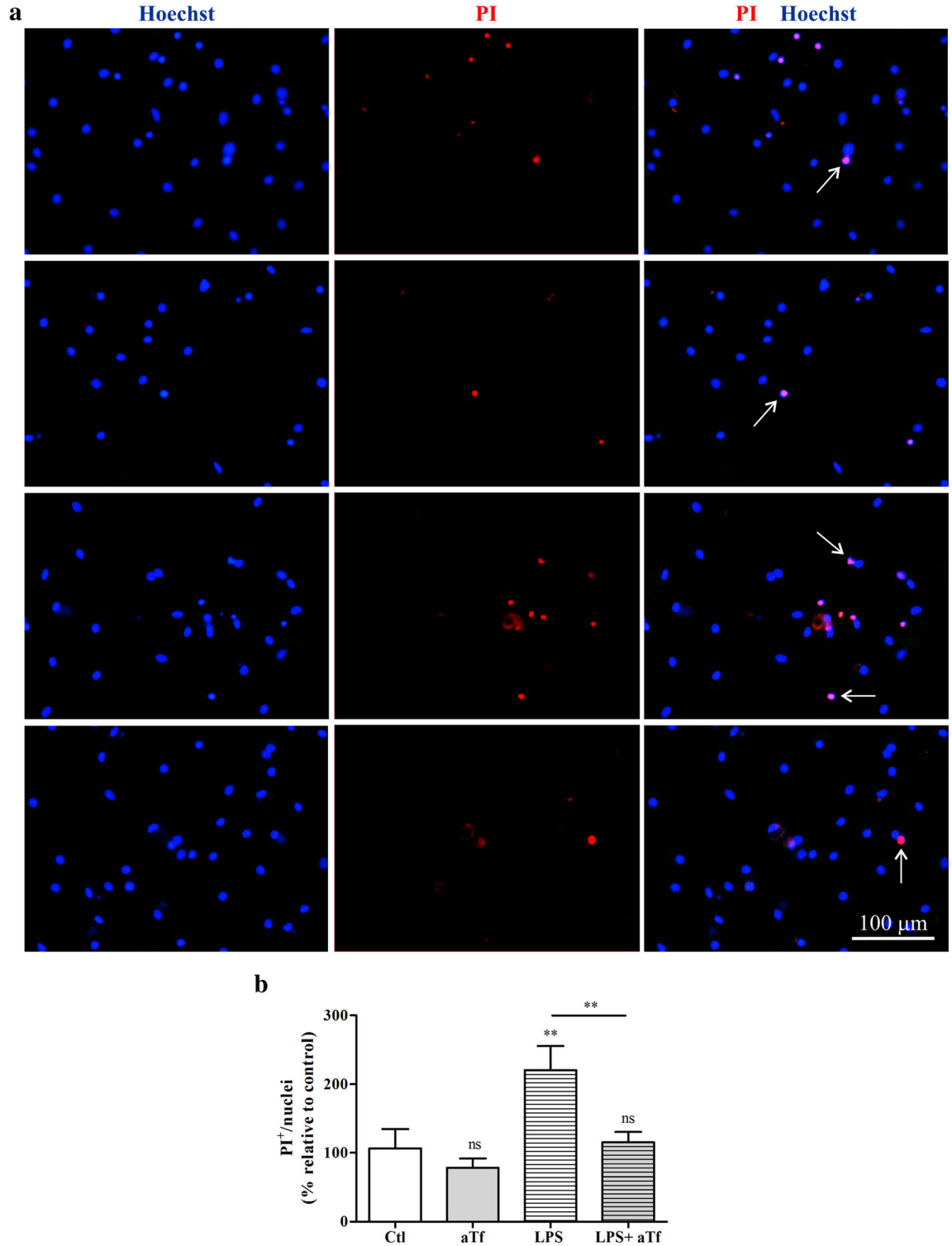

Fig. 7 Microglial cell death upon aTf treatment. **a** Immunofluorescence analysis of PI incorporation (red) in microglial cultures after 48 h of aTf treatment in the presence or absence of LPS; nuclear staining using Hoechst (blue). PI^+/Hoechst cells are indicated with arrows. Scale bar, 200 µm for all images in the panel. **b** Quantification of PI^+ cells relative to total nuclei. Data are presented as the mean ± SEM of three independent experiments using one-way ANOVA followed by Neuman-Keuls multiple comparison test; $^{**}p < 0.01$, ns non-significant, symbols above the bars indicate significance compared to corresponding control. aTf: human apotransferrin; Ctl: control; LPS: lipopolysaccharide; PI: propidium iodide

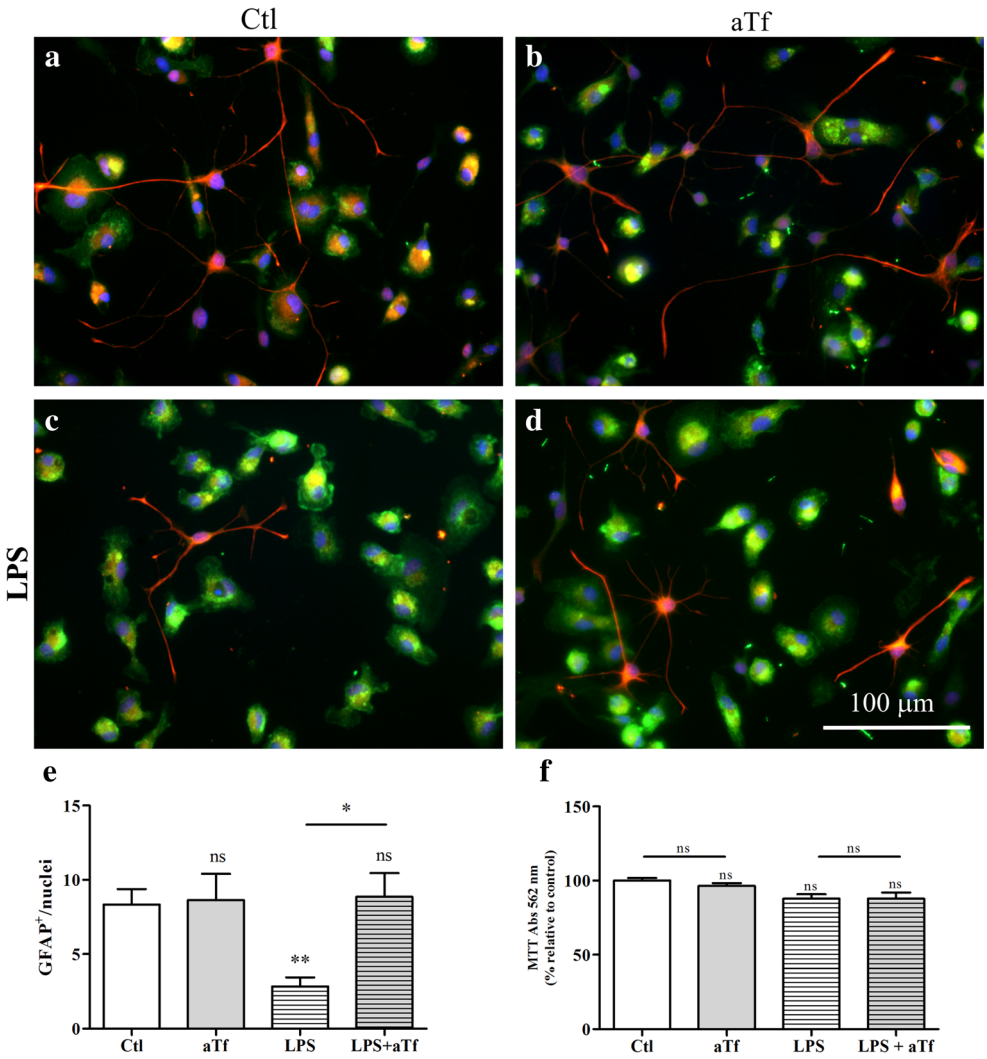

Fig. 8 Astrocyte survival upon aTf treatment of activated microglia. **a** to **d** Immunocytochemical analyses of microglial cultures after 48 h of aTf treatment in the presence or absence of LPS using astrocyte marker GFAP (red) and microglial marker CD11b (green); nuclear staining using Hoechst (blue). Images show fields which contain $GFAP^+$ cells which are not representative of its percentage in the culture. Scale bar, 100 µm for all images. **e** Quantification of $GFAP^+$ cells relative to total nuclei. **f** MTT assays in pure astroglial cultures after 48 h of aTf treatment in the presence or absence of LPS. Data are presented as the mean ± SEM of three independent experiments using one-way ANOVA followed by Neuman-Keuls multiple comparison test; $^{**}p < 0.01$, $^{*}p < 0.05$, ns non-significant, symbols above the bars indicate significance compared to corresponding control. aTf: human apotransferrin; Ctl: control; GFAP: glial fibrillary acidic protein; LPS: lipopolysaccharide

were detected between neighboring cells, especially in the presence of LPS (Fig.10h–k).LPS also produced a significant increase in nitrite production and release to the culture medium as compared to control cells (92.28%, $p < 0.01$), which was again compensated by the presence of aTf (Fig. 10m).

Discussion

Microglia are the brain-resident cells of the innate immune system, and their overactivation is associated with neurodegenerative processes. The control of microglial properties sparks great interest due to the possible therapeutic applications which contemplate stimulating or inducing the cellular mechanisms involved in regeneration, applicable to different pathologies of the CNS [19].

MS is a chronic inflammatory CNS disease which leads to demyelination and neurodegeneration [19, 49, 50]. After demyelination, OPC are recruited to the lesion zone, where they differentiate into mature remyelinating OLG. CPZ administration is an animal model of MS used in rats and mice and characterized by massive demyelination, astrogliosis, and microgliosis [51–53]. This process is spontaneously reversed when CPZ is withdrawn from the diet, which allows the study of in vivo repair mechanisms [29, 53–57].

Treatment of CPZ-fed rats with a single ICI of 350 ng aTf at the time of CPZ withdrawal is known to induce a marked increase in myelin deposition, which results in significantly improved remyelination reflected by histological, immunocytochemical, and biochemical parameters [53]. These results postulate Tf as an active promyelinating agent which could prove key in the treatment of certain demyelinating conditions. Positive effects on myelination and remyelination have allowed us to define aTf as a trophic factor in the CNS.

Our current results demonstrate that, upon CNS demyelinating injury induced in rats by CPZ, OPC, astrocytes, and microglia can incorporate Tf. At the same time, in vitro studies conducted in glial primary cultures show that microglial cells

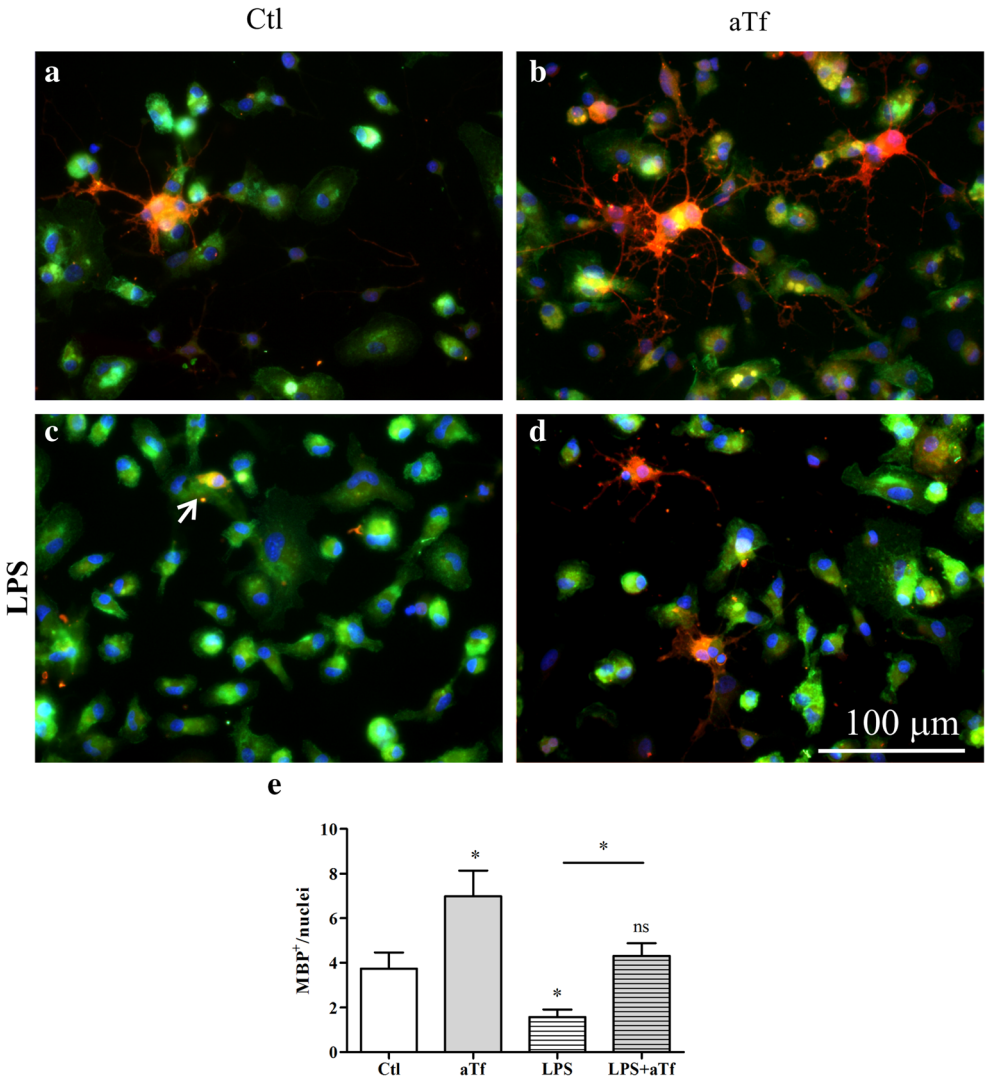

Fig. 9 Oligodendroglial survival upon aTf treatment of activated microglia. **a** to **d** Immunocytochemical analyses of microglial cultures after 48 h of treatment in the presence or absence of LPS using oligodendroglial marker MBP (red) and microglial marker CD11b (green); nuclear staining using Hoechst (blue). Images show fields which contain positive cells which are not representative of its percentage in the culture. Small MBP^+ cell is indicated with arrow (image C). Scale bar, 100 µm for all images. **e** Quantification of MBP^+ cells relative to total nuclei. Data are presented as the mean ± SEM of two independent experiments using one-way ANOVA followed by Neuman-Keuls multiple comparison test; $*p < 0.05$, ns non-significant, symbols above the bars indicate significance compared to corresponding control. aTf: human apotransferrin; Ctl: control; LPS: lipopolysaccharide; MBP: myelin basic protein.

actually incorporate Tf, express TfR, and undergo significant changes upon treatment with Tf in the presence of LPS, such as an increase in proliferation, a sharp expansion in their phagocytic capacity, and a reduction in NO release to values similar to control.

The mechanisms underlying remyelination failure in MS patients are still to be elucidated, although special attention has been paid to the fact that MS lesions, for example, contain numerous OPC which have a potential capacity to myelinate but fail to differentiate into mature OLG. One of the reasons associated with this failure is the presence of myelin debris in the lesion area, which contains inhibitors of OPC differentiation [58–60]. In the intact CNS, inhibitors present in myelin prevent OPC from differentiating in the absence of exposed axons, which could induce OPC apoptosis [61]. Inhibitor removal from the extracellular space is therefore essential during demyelination, in order to prevent interference with the final differentiation of OPC and consequently with the process of remyelination [60].

Fig. 10 Microglial phagocytic capacity and total nitrite release upon aTf treatment. **a**–**d**. Immunocytochemical analyses of phagocytic capacity in microglial cultures incubated with yeasts *Saccharomyces cerevisiae* using FITC (green) for 30 min at 37 °C after 48 h of aTf treatment in the presence or absence of LPS; nuclear staining using Hoechst (blue). The cell shape generated by the phagocytic *Saccharomyces cerevisiae* is indicated with arrows (images A-D). Scale bar, 100 µm for A-D images. **e**–**g** Control immunocytochemical analysis of phagocytic capacity using Cyt B to inhibit actin filament polymerization or at 4 °C. Scale bar, 100 µm for images **e**–**g** images. Immunofluorescence analyses of yeast phagocytosis after 48 h of treatment in **h** Ctl, **i** aTf, **j** LPS, and **k** aTf+LPS conditions using yeast-FITC (green) and actin filament marker rhodamine phalloidin (red). Actin cytoskeleton participation in the phagocytic process is indicated with arrowheads and long membrane processes are indicated with arrows (images H-K). Scale bars, 25 µm for images **h**–**k**. **l** Quantification of yeasts incorporated per cell. **m** Quantification of total nitrites released by microglia to the culture medium through Griess' technique after 48 h of treatment. Data are presented as the mean ± SEM of three independent experiments using two-tailed *t*-test and one-way ANOVA followed by Neuman-Keuls multiple comparison test; $***p < 0{,}001$, $**p < 0.01$, $*p < 0.05$, ns non-significant, symbols above the bars indicate significance compared to corresponding control. Ctl: control; aTf: human apotransferrin; LPS: lipopolysaccharide; Cyt B: cytochalasin B

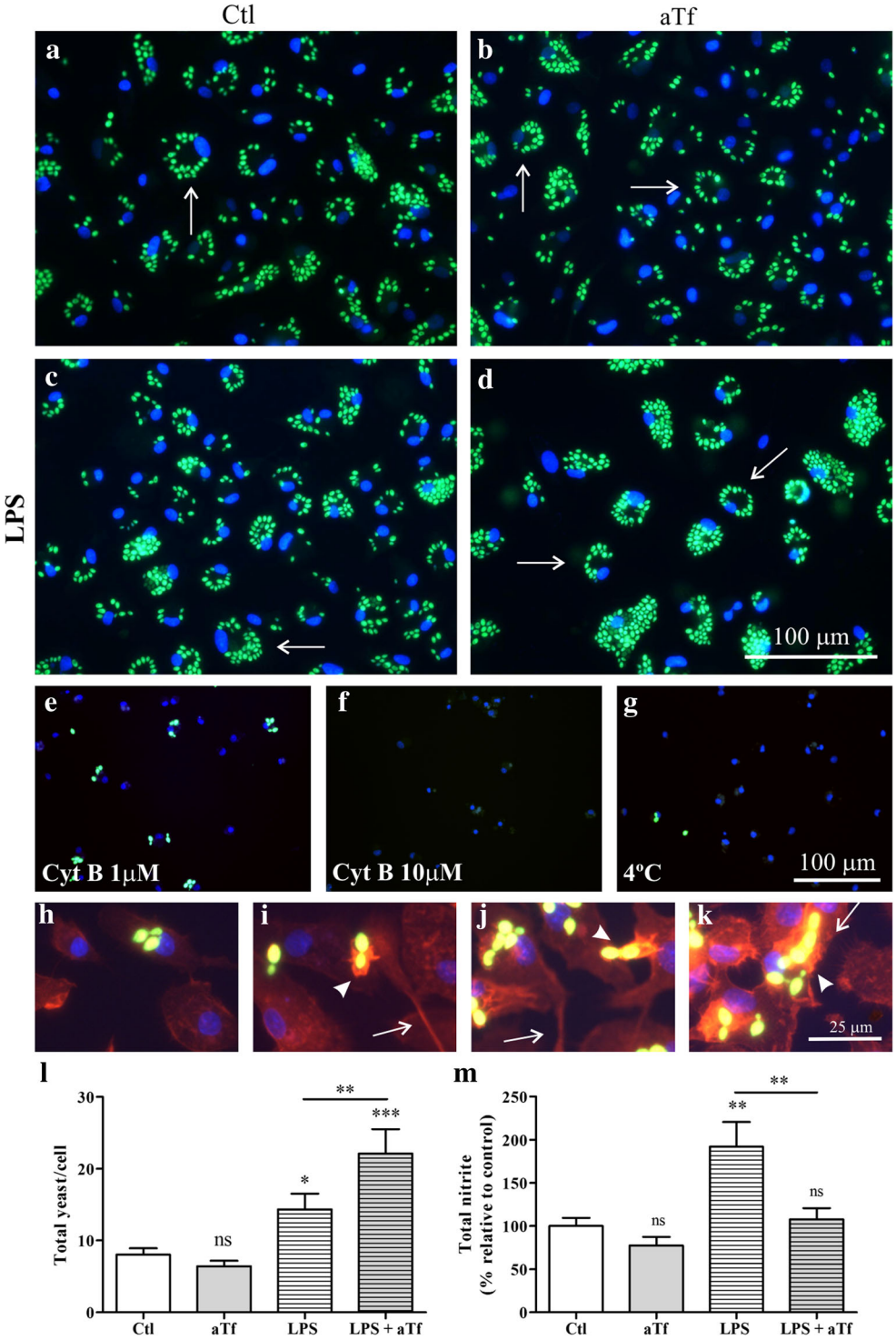

When microglia adopt an M2c phenotype, they recognize apoptotic cellular material through phosphatidylserine [62] or TREM2 receptors [63] and produce an anti-inflammatory response, releasing TGF-β and IL-10, stimulating phagocytosis, and, thus, taking part in tissue remodeling and repair [18, 64, 65]. Cytokine release might be the first step in the immune response after CNS lesion for successful restoration, as it may contribute to the creation of a favorable environment for regeneration. Such cytokines attract phagocytes which remove cell debris from lesions, a turning point between demyelination and remyelination. In this context, the increase in microglial phagocytic capacity observed in the current study upon Tf treatment could be a key event in the generation of a favorable environment for remyelination after phagocytosis of

myelin debris [20, 24]. This effect added to the decrease in NO production observed after the use of Tf in vitro shows that activated microglial phenotypes behave differently in the presence or absence of Tf. Furthermore, the reduction in NO release allows us to speculate that Tf modulates the activation of microglia toward a remyelination-associated phenotype, probably M2.

Genome-wide gene expression analysis of microglia from the CC in the mouse CPZ model has demonstrated the existence of a remyelination-associated phenotype already at the onset of demyelination and throughout remyelination [26]. Supporting these findings, recent studies have shown a switch from M1 to M2 both in resident microglia and in macrophages derived from the periphery at the initiation of CNS remyelination [2, 66–69]. Similarly, OLG differentiation has been shown to increase in vitro with M2-conditioned medium and to decrease in vivo following the selective depletion of M2 during remyelination [70].

The current report further shows that OPC incorporate Tf in vivo both in control and CPZ experimental conditions, which shows them as target cells for Tf in normal conditions and during demyelination. These results are in agreement with the effects described for Tf on in vivo OLG maturation [31, 32, 40, 53] and suggest that aTf has a direct maturational effect on OPC through its internalization. Also, previous results from our laboratory indicate that Tf stimulation of neural and OLG proliferation could be related to their capacity of self-renewal [71]. Furthermore, besides its effects on experimental autoimmune encephalomyelitis progression through the modulation of iron concentration, which leads to the attenuation of reactive microglia and the production of proinflammatory mediators, aTf also shows inhibitory effects on IL-2 production in activated T cells [72]. Worth pointing out, an increase in TfR and ferritin has been detected in MS patients [73].

The repair process associated with the activation of OPC after injury is conditioned by important genetic changes. For example, transcription factors TCF7L2 and SOX2 are expressed only after tissue injury, conditioning the proliferation of OPC and the ability of these cells to differentiate [74, 75]. Although the activation mechanisms of OPC are not completely known, it has been postulated that the first step for this process is the recognition of tissue injury by innate immunity, represented by microglia in the CNS.

The activation of microglia induces the release of several molecules which activate astrocytes by secreting a wide range of factors capable of modifying injured tissue and thus conditioning the proliferation, migration, and differentiation of OPC [19, 76]. The role of astrocytes during de- and remyelination is controversial, and both beneficial and detrimental effects have been reported [28, 29]. It has recently been shown in mice that neuroinflammation mediated by LPS and ischemia induce two different types of reactive astrocytes termed A1 and A2. A1 astrocytes induce the death of neurons and OLG and might be regarded as harmful, while A2 astrocytes upregulate many neurotrophic factors and are thus postulated as protective. A1 astrocytes are induced via the secretion of IL-1α, TNF-α, and C1q by reactive microglia [77]. These findings allow us to hypothesize that the changes in microglial phenotypes induced by Tf could also limit the development of A1 astrocytes, favoring the development of an A2 phenotype.

While OPC and microglia express type 1 TfR [78], astrocytes lack type 1 TfR expression and have been postulated to incorporate iron through Tf-TfR-independent mechanisms [79–82]. Overall, these results indicate that Tf could promote remyelination in vivo by acting, on the one hand, on different cell types able to incorporate Tf, a direct mechanism stimulating OPC maturation and, on the other hand, through uptake by microglia which indirectly participate in OLG maturation by modifying the extracellular milieu and making it suitable for OPC differentiation.

Altogether, our results show the participation of Tf in the modulation of microglial activation and its effects on astrocytic and oligodendroglial cell populations in vitro. Our results also allow us to speculate that this mechanism underlies the effect of aTf on OLG maturation. In sum, the present work contributes to the description of the first impact of extracellular Tf on microglia and provides insights into the favorable microenvironment generated by aTf for the CNS regeneration process.

Acknowledgments The authors are grateful to Dr. Lucas Silvestroff for insightful comments and helpful discussions on this manuscript and María Marta Rancez for the revision of English spelling, grammar, and style in the manuscript.

Funding Sources This work was supported by grants from the Agencia Nacional de Promoción Científica y Tecnológica (BID- PICT 2015-0503) and the University of Buenos Aires (UBA).

References

1. Ransohoff RM, Brown MA (2012) Innate immunity in the central nervous system. J Clin Invest 122(4):1164–1171. https://doi.org/10.1172/JCI58644
2. Davies CL, Miron VE (2018) Distinct origins, gene expression and function of microglia and monocyte-derived macrophages in CNS myelin injury and regeneration. Clin Immunol 189:57–62. https://doi.org/10.1016/j.clim.2016.06.016
3. Parnaik R, Raff MC, Scholes J (2000) Differences between the clearance of apoptotic cells by professional and non-professional phagocytes. Curr Biol 10(14):857–860
4. Calderó J, Brunet N, Ciutat D, Hereu M, Esquerda JE (2009) Development of microglia in the chick embryo spinal cord: implications in the regulation of motoneuronal survival and death. J Neurosci Res 87(11):2447–2466. https://doi.org/10.1002/jnr.22084

5. Kotter MR, Zhao C, van Rooijen N, Franklin RJ (2005) Macrophage-depletion induced impairment of experimental CNS remyelination is associated with a reduced oligodendrocyte progenitor cell response and altered growth factor expression. Neurobiol Dis 18(1):166–175
6. Psachoulia K, Chamberlain KA, Heo D, Davis SE, Paskus JD, Nanescu SE, Dupree JL, Wynn TA et al (2016) IL4I1 augments CNS remyelination and axonal protection by modulating T cell driven inflammation. Brain 139(Pt 12):3121–3136
7. Stevens B, Allen NJ, Vazquez LE, Howell GR, Christopherson KS, Nouri N, Micheva KD, Mehalow AK et al (2007) The classical complement cascade mediates CNS synapse elimination. Cell 131(6):1164–1178
8. Correale J (2014) The role of microglial activation in disease progression. Mult Scler 20(10):1288–1295. https://doi.org/10.1177/1352458514533230
9. Griffin WS, Mrak RE (2002) Interleukin-1 in the genesis and progression of and risk for development of neuronal degeneration in Alzheimer's disease. J Leukoc Biol 72(2):233–238 **Review**
10. Barger SW, Basile AS (2001) Activation of microglia by secreted amyloid precursor protein evokes release of glutamate by cystine exchange and attenuates synaptic function. J Neurochem 76(3):846–854
11. Li Y, Liu L, Barger SW, Mrak RE, Griffin WS (2001) Vitamin E suppression of microglial activation is neuroprotective. J Neurosci Res 66(2):163–170
12. Ajami B, Bennett JL, Krieger C, Tetzlaff W, Rossi FM (2007) Local self-renewal can sustain CNS microglia maintenance and function throughout adult life. Nat Neurosci 10(12):1538–1543
13. Saederup N, Cardona AE, Croft K, Mizutani M, Cotleur AC, Tsou CL, Ransohoff RM, Charo IF (2010) Selective chemokine receptor usage by central nervous system myeloid cells in CCR2-red fluorescent protein knock-in mice. PLoS One 5(10):e13693. https://doi.org/10.1371/journal.pone.0013693
14. Kreutzberg GW (1996) Microglia: a sensor for pathological events in the CNS. Trends Neurosci 8:312–318 Review
15. Stout RD, Jiang C, Matta B, Tietzel I, Watkins SK, Suttles J (2005) Macrophages sequentially change their functional phenotype in response to changes in microenvironmental influences. J Immunol 175(1):342–349
16. Schwartz M, Butovsky O, Brück W, Hanisch UK (2006) Microglial phenotype: is the commitment reversible? Trends Neurosci 29(2):68–74
17. Yamasaki R, Lu H, Butovsky O, Ohno N, Rietsch AM, Cialic R, Wu PM, Doykan CE et al (2014) Differential roles of microglia and monocytes in the inflamed central nervous system. J Exp Med 211(8):1533–1549. https://doi.org/10.1084/jem.20132477
18. Miron VE, Boyd A, Zhao JW, Yuen TJ, Ruckh JM, Shadrach JL, van Wijngaarden P, Wagers AJ et al (2013) M2 microglia and macrophages drive oligodendrocyte differentiation during CNS remyelination. Nat Neurosci 16(9):1211–1218. https://doi.org/10.1038/nn.3469
19. Franklin RJM, Ffrench-Constant C (2017) Regenerating CNS myelin - from mechanisms to experimental medicines. Nat Rev Neurosci 18(12):753–769. https://doi.org/10.1038/nrn.2017.136
20. Ravichandran KS (2003) "Recruitment signals" from apoptotic cells: invitation to a quiet meal. Cell 113(7):817–820
21. Edwards JP, Zhang X, Frauwirth KA, Mosser DM (2006) Biochemical and functional characterization of three activated macrophage populations. J Leukoc Biol 80(6):1298–1307
22. Mantovani A, Sica A, Sozzani S, Allavena P, Vecchi A, Locati M (2004) The chemokine system in diverse forms of macrophage activation and polarization. Trends Immunol 25(12):677–686
23. Mosser DM, Edwards JP (2008) Exploring the full spectrum of macrophage activation. Nat Rev Immunol 8(12):958–969. https://doi.org/10.1038/nri2448
24. Neumann H, Kotter MR, Franklin RJ (2009) Debris clearance by microglia: an essential link between degeneration and regeneration. Brain 132(Pt 2):288–295. https://doi.org/10.1093/brain/awn109.
25. Fancy SP, Kotter MR, Harrington EP, Huang JK, Zhao C, Rowitch DH, Franklin RJ (2010) Overcoming remyelination failure in multiple sclerosis and other myelin disorders. Exp Neurol 225(1):18–23. https://doi.org/10.1016/j.expneurol.2009.12.020
26. Olah M, Amor S, Brouwer N, Vinet J, Eggen B, Biber K, Boddeke HW (2012) Identification of a microglia phenotype supportive of remyelination. Glia 60(2):306–321. https://doi.org/10.1002/glia.21266
27. Ludwin SK, VTs R, Moore CS, Antel JP (2016) Astrocytes in multiple sclerosis. Mult Scler 22(9):1114–1124. https://doi.org/10.1177/1352458516643396 Review
28. Williams A, Piaton G, Lubetzki C (2007) Astrocytes–friends or foes in multiple sclerosis? Glia 55(13):1300–1312 Review
29. Skripuletz T, Wurster U, Worthmann H, Heeren M, Schuppner R, Trebst C, Kielstein JT, Weissenborn K et al (2013) Blood-cerebrospinal fluid barrier dysfunction in patients with neurological symptoms during the 2011 Northern German E. coli serotype O104:H4 outbreak. Brain 136(Pt 8):e241. https://doi.org/10.1093/brain/aws361
30. Bartlett WP, Li XS, Connor JR (1991) Expression of transferrin mRNA in the CNS of normal and jimpy mice. J Neurochem 57(1):318–322
31. Escobar Cabrera OE, Bongarzone ER, Soto EF, Pasquini JM (1994) Single intracerebral injection of apotransferrin in young rats induces increased myelination. Dev Neurosci 16(5–6):248–254
32. Escobar Cabrera OE, Zakin MM, Soto EF, Pasquini JM (1997) Single intracranial injection of apotransferrin in young rats increases the expression of specific myelin protein mRNA. J Neurosci Res 47(6):603–608
33. Escobar Cabrera OE, Soto EF, Pasquini JM (2000) Myelin membranes isolated from rats intracranially injected with apotransferrin are more susceptible to in vitro peroxidation. Neurochem Res 25(1):87–93
34. Marta CB, Paez P, Lopez M, Pellegrino de Iraldi A, Soto EF, Pasquini JM (2003) Morphological changes of myelin sheaths in rats intracranially injected with apotransferrin. Neurochem Res 28(1):101–110
35. Paez PM, Marta CB, Moreno MB, Soto EF, Pasquini JM (2002) Apotransferrin decreases migration and enhances differentiation of oligodendroglial progenitor cells in an in vitro system. Dev Neurosci 24(1):47–58
36. Paez PM, García CI, Davio C, Campagnoni AT, Soto EF, Pasquini JM (2004) Apotransferrin promotes the differentiation of two oligodendroglial cell lines. Glia 46(2):207–217
37. Espinosa de los Monteros A, Peña LA, de Vellis J (1989) Does transferrin have a special role in the nervous system? J Neurosci Res 24(2):125–136 Review
38. Espinosa de los Monteros A, Kumar S, Zhao P, Huang CJ, Nazarian R, Pan T, Scully S, Chang R et al (1999) Transferrin is an essential factor for myelination. Neurochem Res 24(2):235–248
39. Espinosa-Jeffrey A, Kumar S, Zhao PM, Awosika O, Agbo C, Huang A, Chang R, De Vellis J (2002) Transferrin regulates transcription of the MBP gene and its action synergizes with IGF-1 to enhance myelinogenesis in the md rat. Dev Neurosci 24(2–3):227–241
40. Franco PG, Pasquini LA, Pérez MJ, Rosato-Siri MV, Silvestroff L, Pasquini JM (2015) Paving the way for adequate myelination: The contribution of galectin-3, transferrin and iron. FEBS Lett 589(22):3388–3395
41. Perez MJ, Ortiz EH, Roffé M, Soto EF, Pasquini JM (2009) Fyn kinase is involved in oligodendroglial cell differentiation induced by apotransferrin. J Neurosci Res 87(15):3378–3389
42. Paxinos G, Watson C (1998) The rat brain in stereotaxic coordinates. Academic Press, San Diego

43. McCarthy KD, de Vellis J (1980) Preparation of separate astroglial and oligodendroglial cell cultures from rat cerebral tissue. J Cell Biol 85(3):890–902
44. Griess P (1879) BemerkungenzuderAbhandlung der HH.Weselsky und BenediktUebereinigeAzoverbindungen. Ber Dtsch Chem Ges 12(1879):426–428
45. Lee SJ, So IS, Park SY, Kim IS (2008) Thymosin beta4 is involved in stabilin-2-mediated apoptotic cell engulfment. FEBS Lett 582(15):2161–2166. https://doi.org/10.1016/j.febslet.2008.03.058
46. Schrijvers DM, Martinet W, De Meyer GR, Andries L, Herman AG, Kockx MM (2004) Flow cytometric evaluation of a model for phagocytosis of cells undergoing apoptosis. J Immunol Methods 287(1–2):101–108
47. Ribes S, Ebert S, Regen T, Agarwal A, Tauber SC, Czesnik D, Spreer A, Bunkowski S et al (2010) Toll-like receptor stimulation enhances phagocytosis and intracellular killing of nonencapsulated and encapsulated *Streptococcus pneumoniae* by murine microglia. 78(2):865–871. https://doi.org/10.1128/IAI.01110-09
48. Oberhammer F, Fritsch G, Schmied M, Pavelka M, Printz D, Purchio T, Lassmann H, Schulte-Hermann R (1993) Condensation of the chromatin at the membrane of an apoptotic nucleus is not associated with activation of an endonuclease. J Cell Sci 104(Pt 2):317–326
49. Compston A, Coles A (2008) Multiple sclerosis. Lancet 372(9648): 1502–1517. https://doi.org/10.1016/S0140-6736(08)61620-7
50. Lassmann H, van Horssen J (2011) The molecular basis of neurodegeneration in multiple sclerosis. FEBS Lett 585(23):3715–3723. https://doi.org/10.1016/j.febslet.2011.08.004. Review.
51. Johnson ES, Ludwin SK (1981) The demonstration of recurrent demyelination and remyelination of axons in the central nervous system. Acta Neuropathol 53(2):93–98
52. Kondo A, Nakano T, Suzuki K (1987) Blood-brain barrier permeability to horseradish peroxidase in twitcher and cuprizone-intoxicated mice. Brain Res 425(1):186–190
53. Adamo AM, Paez PM, Escobar Cabrera OE, Wolfson M, Franco PG, Pasquini JM, Soto EF (2006) Remyelination after cuprizone-induced demyelination in the rat is stimulated by apotransferrin. Exp Neurol 198(2):519–529
54. Matsushima GK, Morell P (2001) Theneurotoxicant, cuprizone, as a model to study demyelination and remyelination in the central nervous system. Brain Pathol 11(1):107–116 Review
55. McMahon EJ, Suzuki K, Matsushima GK (2002) Peripheral macrophage recruitment in cuprizone-induced CNS demyelination despite an intact blood-brain barrier. J Neuroimmunol 130(1–2):32–45
56. Remington LT, Babcock AA, Zehntner SP, Owens T (2007) Microglial recruitment, activation, and proliferation in response to primary demyelination. Am J Pathol 170(5):1713–1724
57. Kipp M, Clarner T, Dang J, Copray S, Beyer C (2009) The cuprizone animal model: new insights into an old story. Acta Neuropathol 118(6):723–736. https://doi.org/10.1007/s00401-009-0591-3 Review
58. Kotter MR, Li WW, Zhao C, Franklin RJ (2006) Myelin impairs CNS remyelination by inhibiting oligodendrocyte precursor cell differentiation. J Neurosci 26(1):328–332
59. Syed YA, Baer AS, Lubec G, Hoeger H, Widhalm G, Kotter MR (2008) Inhibition of oligodendrocyte precursor cell differentiation by myelin-associated proteins. Neurosurg Focus 24(3–4):E5. https://doi.org/10.3171/FOC/2008/24/3-4/E4
60. Lampron A, Larochelle A, Laflamme N, Préfontaine P, Plante MM, Sánchez MG, Yong VW, Stys PK et al (2015) Inefficient clearance of myelin debris by microglia impairs remyelinating processes. Exp Med 212(4):481–495. https://doi.org/10.1084/jem.20141656
61. Plemel JR, Manesh SB, Sparling JS, Tetzlaff W (2013) Myelin inhibits oligodendroglial maturation and regulates oligodendrocytic transcription factor expression. Glia 61(9):1471–1487. https://doi.org/10.1002/glia.22535
62. Grommes C, Lee CY, Wilkinson BL, Jiang Q, Koenigsknecht-Talboo JL, Varnum B, Landreth GE (2008) Regulation of microglial phagocytosis and inflammatory gene expression by Gas6 acting on the Axl/Mer family of tyrosine kinases. J NeuroImmune Pharmacol 3(2):130–140. https://doi.org/10.1007/s11481-007-9090-2
63. Hsieh CL, Koike M, Spusta SC, Niemi EC, Yenari M, Nakamura MC, Seaman WE (2009) A role for TREM2 ligands in the phagocytosis of apoptotic neuronal cells by microglia. J Neurochem 109(4):1144–1156. https://doi.org/10.1111/j.1471-4159.2009.06042.x
64. Mantovani A, Sica A, Locati M (2005) Macrophage polarization comes of age. Immunity 23(4):344–346 **Review**
65. Geissmann F, Manz MG, Jung S, Sieweke MH, Merad M, Ley K (2010) Development of monocytes, macrophages, and dendritic cells. Science 327(5966):656–661. https://doi.org/10.1126/science.1178331
66. Yu Z, Sun D, Feng J, Tan W, Fang X, Zhao M, Zhao X, Pu Y et al (2015) MSX3 switches microglia polarization and protects from inflammation-induced demyelination. J Neurosci 35(16):6350–6365. https://doi.org/10.1523/JNEUROSCI.2468-14.2015
67. Rawji KS, Mishra MK, Yong VW (2016) Regenerative capacity of macrophages for remyelination. Front Cell Dev Biol 4:47
68. Sun D, Yu Z, Fang X, Liu M, Pu Y, Shao Q, Wang D, Zhao X et al (2017) LncRNA GAS5 inhibits microglial M2 polarization and exacerbates demyelination. EMBO Rep 18(10):1801–1816. https://doi.org/10.15252/embr.201643668
69. Kalakh S, Mouihate A (2017) Androstenediol reduces demyelination-induced Axonopathy in the rat corpus callosum: impact on microglial polarization. Front Cell Neurosci 23(11):49. https://doi.org/10.3389/fncel.2017.00049.
70. Miron VE (2013) Dissecting the damaging versus regenerative roles of CNS macrophages: implications for the use of immunomodulatory therapeutics. Regen Med 8(6):673–676. https://doi.org/10.2217/rme.13.73 Review
71. Silvestroff L, Franco PG, Pasquini JM (2013) Neural and oligodendrocyte progenitor cells: transferrin effects on cell proliferation. ASN Neuro 5(1):e00107. https://doi.org/10.1042/AN20120075.
72. Saksida T, Miljkovic D, Timotijevic G, Stojanovic I, Mijatovic S, Fagone P, Mangano K, Mammana S et al (2013) Apotransferrin inhibits interleukin-2 expression and protects mice from experimental autoimmune encephalomyelitis. J Neuroimmunol 262(1–2):72–78. https://doi.org/10.1016/j.jneuroim.2013.07.001
73. Sfagos C, Makis AC, Chaidos A, Hatzimichael EC, Dalamaga A, Kosma K, Bourantas KL (2005) Serum ferritin, transferrin and soluble transferrin receptor levels in multiple sclerosis patients. Mult Scler 11(3):272–275
74. Fancy SP, Baranzini SE, Zhao C, Yuk DI, Irvine KA, Kaing S, Sanai N, Franklin RJ et al (2009) Dysregulation of the Wnt pathway inhibits timely myelination and remyelination in the mammalian CNS. Genes Dev 23(13):1571–1585. https://doi.org/10.1101/gad.1806309
75. Zhao C, Ma D, Zawadzka M, Fancy SP, Elis-Williams L, Bouvier G, Stockley JH, de Castro GM et al (2015) Sox2 sustains recruitment of oligodendrocyte progenitor cells following CNS demyelination and primes them for differentiation during remyelination. J Neurosci 35(33):11482–11499. https://doi.org/10.1523/JNEUROSCI.3655-14.2015
76. Franklin RJ, ffrench-Constant C, Edgar JM, Smith KJ (2012) Neuroprotection and repair in multiple sclerosis. Nat Rev Neurol 8(11):624–634. https://doi.org/10.1038/nrneurol.2012.200
77. Liddelow SA, Guttenplan KA, Clarke LE, Bennett FC, Bohlen CJ, Schirmer L, Bennett ML, Münch AE et al (2017) Neurotoxic reactive astrocytes are induced by activated microglia. Nature 541(7638):481–487. https://doi.org/10.1038/nature21029

78. McCarthy RC, Sosa JC, Gardeck AM, Baez AS, Lee CH, Wessling-Resnick MJ (2018) Inflammation-induced iron transport and metabolism by brain microglia. Biol Chem 293(20):7853–7863. https://doi.org/10.1074/jbc.RA118.001949
79. Connor JR, Benkovic SA (1992) Iron regulation in the brain: histochemical, biochemical, and molecular considerations. Ann Neurol 32(Suppl):S51–S61 Review
80. Suzumura A, Sawada M, Mokuno K, Kato K, Marunouchi T, Yamamoto H (1993) Effects of microglia-derived cytokines on astrocyte proliferation. Restor Neurol Neurosci 5(5):347–352. https://doi.org/10.3233/RNN-1993-55605
81. Moos T (1996) Immunohistochemical localization of intraneuronal transferrin receptor immunoreactivity in the adult mouse central nervous system. J Comp Neurol 375(4):675–692
82. Leitner DF, Connor JR (2012) Functional roles of transferrin in the brain. Biochim Biophys Acta 1820(3):393–402. https://doi.org/10.1016/j.bbagen.2011.10.016 Review